

Determination of Electron and Hole Capture Rates in Nickel-Doped Germanium Using Photomagnetolectric and Photoconductive Methods

H. F. Tseng and S. S. Li

Department of Electrical Engineering, University of Florida, Gainesville, Florida 32601

(Received 18 February 1972)

Although room-temperature electron and hole capture rates for nickel atoms in germanium have been previously reported, no conclusive result has as yet been reached. This is due to the fact that carrier capture rates for nickel-doped germanium reported previously were determined mainly from the temperature dependence of lifetimes, which is further complicated and prone to obtain incorrect results when the capture rates become temperature dependent. In this paper, we have demonstrated that by including the excess-carrier trapping effect in the theory of photomagnetolectric (PME) and photoconductive (PC) effects and by elaborately controlling the compensation ratio of nickel and shallow-impurity densities in germanium, we are able to determine accurately three of the four capture rates for nickel atoms in germanium from room-temperature PME and PC measurements. In addition, with the present results, we are able to interpret the previous results consistently at room temperature. The present results are $C_{n1} = 1.4 \times 10^{-9}$, $C_{n2} = 8 \times 10^{-9}$, and $C_{p2} = 4 \times 10^{-8}$ in units of $\text{cm}^3 \text{sec}^{-1}$ at $T = 300^\circ\text{K}$.

I. INTRODUCTION

It is known that a substitutional nickel atom introduces, in agreement with the tetrahedral-covalent-bond model, two acceptor levels in the forbidden band of germanium. One of them is located at 0.30 eV below the conduction-band edge, and the other is 0.22 eV above the valence-band edge; both levels are known to serve as efficient recombination centers. Nickel atoms can be introduced into germanium crystal by ordinary diffusion process.

The properties of nickel-doped germanium have received considerable attention since the recombination property was first investigated by Burton *et al.*¹ They were able to interpret the electron-hole recombination in terms of the first acceptor level. Tyler *et al.*² later found the second acceptor level, but failed to show that both levels were associated with the same substitutional nickel atom. Subsequently, Battey and Baum,³ in a study of the temperature dependence of lifetime, deduced the electron capture rates in both levels. They found that C_{n1} was independent of the temperature, while C_{n2} increased exponentially with temperature. On the other hand, Okada⁴ showed that photoconductivity in nickel-doped germanium crystals can be interpreted in terms of the temperature-independent capture rates C_{n2} and C_{p2} ; Kalashnikov and Tissen⁵ showed that the photomagnetolectric (PME) lifetime in *p*-type crystals can be interpreted in terms of a two-level model assuming that C_{n1} and C_{n2} are independent of temperature and have a ratio of $C_{n1}/C_{n2} = 6$. However, Wertheim,⁶ in his study of the bombardment-conductivity decay-time experiments, concluded that C_{n1} and C_{n2} are in-

dependent of temperature but with the ratio $C_{n1}/C_{n2} = \frac{1}{6}$, which is contradictory to the result of Kalashnikov and Tissen.⁵ This discrepancy was later explained by Eliseev and Kalashnikov⁷ as due to dislocations in their early germanium crystals, and they concluded that C_{n2} is larger than C_{n1} with the ratio $C_{n1}/C_{n2} = \frac{1}{6}$.

Note that the ratios of electron capture rates C_{n1}/C_{n2} reported by Wertheim⁶ and Eliseev *et al.*⁷ are consistent at room temperature (i. e., $C_{n1}/C_{n2} = \frac{1}{6}$). However, the values of C_{n1} and C_{n2} reported by Eliseev *et al.* are a factor of 2 smaller than that of Wertheim (see Table I). The values of hole capture rates reported by previous authors are even more widely spread and less conclusive. The main reason for this is the fact that most of these results are determined from the temperature dependence of lifetimes, which is further complicated and prone to lead to incorrect results if some of the recombination parameters (e. g., capture rates) become temperature dependent.

In this paper, we shall demonstrate that by including the excess-carrier trapping effect in the theory of photomagnetolectric (PME) and photoconductive (PC) effects and by elaborately controlling the compensation ratio of nickel and

TABLE I. Capture rates for nickel atoms in germanium (in units of $10^{-9} \text{ cm}^3 \text{ sec}^{-1}$), $T = 300^\circ\text{K}$.

Refs.	C_{n1}	C_{n2}	C_{p1}	C_{p2}
Burton <i>et al.</i> (Ref. 1)	0.8	>40
Wertheim (Ref. 6)	0.96	5.9	...	~100
Eliseev and Kalashnikov (Ref. 7)	0.5	3
This paper	1.4	8	...	40

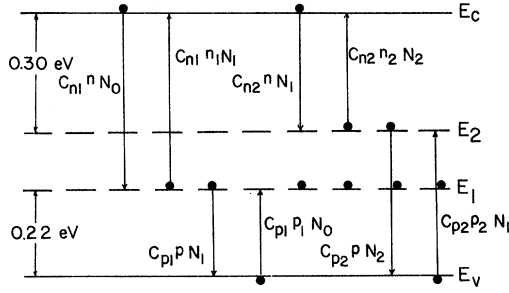


FIG. 1. Energy-band diagram for nickel-doped germanium; the transitions between the bands and the two nickel acceptor levels are shown.

shallow-impurity densities in germanium, we are able to determine carrier capture rates more accurately at room temperature from PME and PC measurements. Furthermore, by closely examining the previous results, we are able to interpret the present results consistently with those reported by Wertheim and Eliseev *et al.*

II. THEORY

The energy levels of nickel atoms in germanium and the transitions among bands and the nickel levels are shown schematically in Fig. 1. The nickel atoms in the three possible charge states (with zero, one, and two electrons in the two acceptor levels of nickel atoms) are designated by N_0 , N_1 , and N_2 , which are further related by the totality condition

$$N_0 + N_1 + N_2 = N_i, \quad (1)$$

where N_i is the total concentration of nickel atoms. The parameters n_1 , p_1 , n_2 , and p_2 represent the carrier densities when the Fermi level coincides with acceptor levels E_1 and E_2 , respectively. They are related to the densities of impurity charge states through the following relations⁸:

$$n_1 = n_0 p_0 / p_1 = n_0 e^{(E_1 - E_F) / kT} = n_0 N_0^0 / N_1^0; \quad (2)$$

similarly,

$$n_2 = n_0 e^{(E_2 - E_F) / kT} = n_0 N_1^0 / N_2^0, \quad (3)$$

where we have used the superscript 0 to denote the equilibrium densities, and E_F is the Fermi level. The above equations also provide the relationship of the equilibrium nickel densities in different charge states to the Fermi level. From Eqs. (1)–(3), the density of nickel atoms in each charge state can be determined from the Hall effect and the conductivity experiments.

From Fig. 1, the rate equations in the bands and the nickel acceptor levels can be written as

$$\frac{dn}{dt} = \sum_{j=1}^2 R_{nj} + G, \quad \frac{dp}{dt} = \sum_{j=1}^2 R_{pj} + G,$$

$$\frac{dN_2}{dt} = R_{n2} - R_{p2}, \quad \frac{dN_1}{dt} = R_{n1} - R_{p1} - \frac{dN_2}{dt}, \quad (4)$$

$$R_{n1} = C_{n1} (nN_0 - n_1 N_1), \quad R_{p1} = C_{p1} (pN_1 - p_1 N_0),$$

$$R_{n2} = C_{n2} (nN_1 - n_2 N_2), \quad R_{p2} = C_{p2} (pN_2 - p_2 N_1).$$

The charge-neutrality condition expressed in terms of the excess densities from the equilibrium values is given by

$$\Delta p - \Delta n - \Delta N_1 - 2\Delta N_2 = 0. \quad (5)$$

Under the condition of small injection⁹ (i. e., $\Delta n \ll n_0 + n_j$, $\Delta p \ll p_0 + p_j$, $j = 1, 2$) and the steady-state case, the lifetimes for electrons and holes are defined, respectively, by⁸

$$\tau_n = \Delta n / \sum_{j=1}^2 R_{nj} \quad (6)$$

and

$$\tau_p = \Delta p / \sum_{j=1}^2 R_{pj}. \quad (7)$$

From Eqs. (4)–(7), the trapping ratio Γ and the lifetimes can be expressed by¹⁰

$$\Gamma = \frac{\Delta n}{\Delta p} = \frac{\tau_n}{\tau_p} = \frac{1 - \beta_1 \beta_2 + (1 + \beta_2) \mu_{p1} + (1 + \beta_1) \mu_{p2}}{1 - \beta_1 \beta_2 + (1 + \beta_2) \mu_{n1} + (1 + \beta_1) \mu_{n2}}, \quad (8)$$

$$\begin{aligned} \tau_n^{-1} &= (p_0 + \Gamma^{-1} n_0) [C_{n1} C_{p1} (N_0^0 + N_1^0) / H_1 \\ &\quad + C_{n2} C_{p2} (N_1^0 + N_2^0) / H_2] \\ &= (p_0 + \Gamma^{-1} n_0) \{ [\tau_{p01} (n_0 + n_1) + \tau_{n01} (p_0 + p_1)]^{-1} \\ &\quad + [\tau_{p02} (n_0 + n_2) + \tau_{n02} (p_0 + p_2)]^{-1} \}, \quad (9) \end{aligned}$$

where

$$H_1 = C_{n1} (n_0 + n_1) + C_{p1} (p_0 + p_1), \quad (10)$$

$$H_2 = C_{n2} (n_0 + n_2) + C_{p2} (p_0 + p_2), \quad (11)$$

$$\mu_{n1} = C_{n1} N_0^0 / H_1, \quad \mu_{n2} = C_{n2} N_1^0 / H_2, \quad (12)$$

$$\mu_{p1} = C_{p1} N_1^0 / H_1, \quad \mu_{p2} = C_{p2} N_2^0 / H_2, \quad (13)$$

$$\beta_1 = N_0^0 / (N_0^0 + N_1^0), \quad (14)$$

$$\beta_2 = N_1^0 / (N_1^0 + N_2^0), \quad (15)$$

$$\tau_{n01} = 1 / C_{n1} (N_0^0 + N_1^0), \quad \tau_{n02} = 1 / C_{n2} (N_1^0 + N_2^0), \quad (16)$$

$$\tau_{p01} = 1 / C_{p1} (N_0^0 + N_1^0), \quad \tau_{p02} = 1 / C_{p2} (N_1^0 + N_2^0). \quad (17)$$

For steady-state case, $R_{n1} = R_{p1} = R_1$, $R_{n2} = R_{p2} = R_2$, and the relative importance of the net steady-state recombination rates of the two levels can be obtained from the following expression⁸:

$$\frac{R_2}{R_1} = \frac{C_{n2}(n_0 + p_1 C_{p1}/C_{n1})}{C_{p1}(p_0 + C_{n2}n_2/C_{p2})}. \quad (18)$$

For an n -type sample, $n_0 \gg p_0$, $p_1 C_{p1}/C_{n1} \gg C_{n2}n_2/C_{p2}$, therefore, $R_2 \gg R_1$; the upper level dominates for all temperatures, and the recombination process reduces to the Shockley-Read model for single level.¹¹ Equation (9) then reduces to Eq. (A7) of Ref. 11.

For p -type samples, we find

$$\frac{R_2}{R_1} \approx \frac{C_{n2}}{C_{n1}} \frac{p_1}{p_0}. \quad (19)$$

The relative importance of the two acceptor levels depends on the ratio of C_{n2}/C_{n1} and the resistivity of the samples.

For the case of small injection, by taking into account the trapping effect, the steady-state PME open-circuit voltage can be expressed in terms of the photoconductance¹²:

$$V_{\text{PME}} = \frac{(\theta_n + \theta_p)}{\mu_p (b + \Gamma^{-1})} \left(\frac{n_0 \Gamma^{-1} + p_0}{n_0 b + p_0} \right)^{1/2} \times \left(\frac{D_n}{\tau_n} \right)^{1/2} \left(\frac{\Delta G}{G_0} \right), \quad (20)$$

where V_{PME} is the PME open-circuit voltage per unit length, $\theta_n = \mu_{nH} B$ and $\theta_p = \mu_{pH} B$ are Hall angles for electrons and holes, respectively. ΔG is the photoconductance per unit length-to-width ratio of the sample, and G_0 is the dark conductance. Other parameters not defined here have the conventional meanings. By means of Eqs. (8), (9), and (20), we can compute the capture rates and lifetimes from the PME and PC data.

III. EXPERIMENTAL DETAILS

n -type germanium single crystals were cut into rectangular bars with typical dimensions of $0.8 \times 5 \times 12 \text{ mm}^3$. The shallow-donor densities were determined from the Hall effect and the conductivity measurements. These samples were cleaned by chemical process and coated with nickel by vacuum evaporation. The samples were then placed in the furnace for diffusion. At the end of the diffusion period, the samples were quenched to room temperature. The nickel concentrations were controlled by the diffusion temperature. The nickel-doped sample was mounted in a AC-310 liquid-helium-refrigeration system for measurements. The Hall effect and the conductivity measurements were taken by standard dc technique. The PME and PC measurements were taken by using a chopped light source and an ac detecting system, so that the temperature-gradient effect can be eliminated.

The samples for investigation were divided into two groups: One group has the nickel densities in

the range that $N_i < N_D < 2N_i$; in this way, the nickel-doped germanium samples remained as n type, but with high resistivity. The second group was prepared with $N_i > N_D$, so that samples become p type after nickel diffusion. The nickel densities can be determined accurately from Hall effect and the conductivity measurements. We shall next discuss the results of our measurements on these two groups of samples separately.

n -Type Samples

For this group of samples, the first acceptor levels (i. e., E_1 level) of the nickel atoms are fully occupied by electrons, and the second acceptor levels (i. e., E_2) are partially occupied. The occupation probability of the second level and the densities of nickel in each charge states can be determined from Eq. (3). In order to show that nickel is the only dominant impurity in these samples, we measured the Hall coefficient, electrical resistivity, and electron density as a function of temperature before the PME and PC measurements.

Figure 2 shows the temperature dependence of Hall mobility for temperature between 180 and 300 °K for sample Ge-N2 ($N_D = 3.5 \times 10^{15} \text{ cm}^{-3}$, $N_i = 2 \times 10^{15} \text{ cm}^{-3}$). The Hall mobility is found nearly independent of temperature in this temperature range. The electron drift mobility μ_n can be deduced from the relation that¹³

$$\mu_n = \mu_{nH} R_\infty / R_H.$$

Here μ_{nH} and R_H are the low-field Hall mobility and Hall coefficient, respectively, and R_∞ is the Hall coefficient at very high field. For electrons, this ratio is nearly equal to unity in the temperature range of interest.^{13,14} Figures 3 and 4 illustrate the temperature dependence of resistivity and

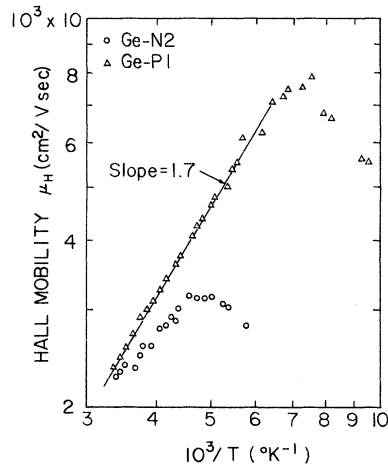


FIG. 2. Hall mobility vs temperature for samples Ge-N2 (with $N_D = 3.5 \times 10^{15} \text{ cm}^{-3}$, $N_i = 2.0 \times 10^{15} \text{ cm}^{-3}$) and Ge-P1 (with $N_D = 1.4 \times 10^{14} \text{ cm}^{-3}$, $N_i = 7.5 \times 10^{14} \text{ cm}^{-3}$).

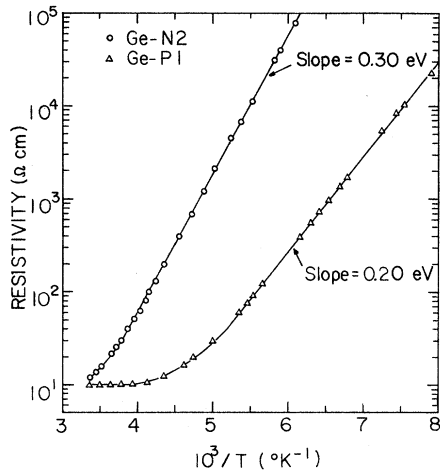


FIG. 3. Resistivity vs temperature for samples Ge-N2 and Ge-P1.

electron concentration, respectively, for sample Ge-N2. Since the electron mobility is nearly independent of temperature, the activation energies deduced from the slope of these two curves are identical and equal to 0.30 eV. This represents the activation energy of the second acceptor level of nickel (i. e., $E_2 = 0.30$ eV below the conduction-band edge).

The PME and PC measurements were taken at room temperature, and the result is displayed in

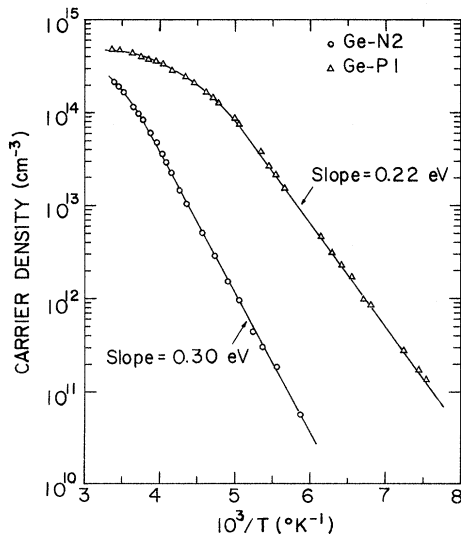


FIG. 4. Carrier densities vs temperature for samples Ge-N2 and Ge-P1. The activation energy for Ge-N2 is found equal to 0.30 eV which is the second acceptor level of the nickel atom in Ge. The activation energy for Ge-P1 is found equal 0.22 eV, which is the first acceptor level of the nickel atom in Ge.

Fig. 5, for $B = 3$ kG.

The linear relationship between V_{PME} and $\Delta G/G_0$, as predicted by Eq. (20), is observed in Fig. 5.

To calculate the recombination parameters from Eqs. (8), (9), and (20), we examined over ten samples with different donor and nickel concentrations. The parameters n_1 , p_1 , n_2 , and p_2 used in computations have the following values at 300 °K:

$$\begin{aligned} n_1 &= 3.0 \times 10^{11} \text{ cm}^{-3}, & p_1 &= 1.2 \times 10^{15} \text{ cm}^{-3}, \\ n_2 &= 9.7 \times 10^{13} \text{ cm}^{-3}, & p_2 &= 3.8 \times 10^{12} \text{ cm}^{-3}. \end{aligned}$$

The electron diffusion coefficient D_n is obtained from μ_n through the use of Einstein's relation that $D_n = (kT/q)\mu_n$. The ratio of electron and hole mobilities is taken from the results reported by Prince.¹⁴

For n -type samples, the upper level is dominant and the lower level has little effect on the trapping ratio Γ (since p_1 is very large); Eqs. (8) and (9) can be simplified into the forms

$$\Gamma = \frac{n_0 + n_2 + \gamma_2(p_0 + p_2 + N_2^0)}{n_0 + n_2 + \gamma_2(p_0 + p_2) + N_1^0} \quad (21)$$

and

$$\tau_n^{-1} = (p_0 + \Gamma^{-1}n_0) / [\tau_{p02}(n_0 + n_2) + \tau_{n02}(p_0 + p_2)], \quad (22)$$

where $\gamma_2 = C_{p2}/C_{n2}$, and τ_{n02} and τ_{p02} are given by Eqs. (16) and (17). From Eqs. (20) and (22), it is noted that V_{PME} and τ_n^{-1} depend greatly on the trapping ratio Γ which in turn depends on the ratio γ_2 .

From the present experimental data, we can calculate γ_2 as well as C_{n2} and C_{p2} . The result yields

$$\begin{aligned} \gamma_2 &= 5, \\ C_{n2} &= 8 \times 10^{-9} \text{ cm}^3/\text{sec}, \end{aligned}$$

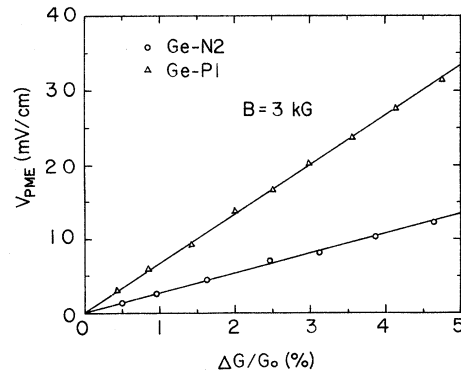


FIG. 5. PME open-circuit voltage V_{PME} vs photoconductance $\Delta G/G_0$ for samples Ge-N2 and Ge-P1, for $B = 3$ kG.

$$C_{p2} = 40 \times 10^{-9} \text{ cm}^3/\text{sec}.$$

For comparison, we summarize our results together with the results reported by other investigators in Table I.

p-Type Samples

For this group of samples, the first acceptor levels (i. e., E_1) are partially occupied, and the second acceptor levels are completely empty. The results are shown in Figs. 2-5 for sample Ge-P1 (with $N_D = 1.4 \times 10^{14} \text{ cm}^{-3}$, $N_i = 7.5 \times 10^{14} \text{ cm}^{-3}$). Figure 2 shows the hole Hall mobility versus temperature. The temperature dependence of the hole Hall mobility is found to be $T^{-1.7 \pm 0.02}$ which is in good agreement with $T^{-1.6}$ dependence of hole mobility reported by Prince.¹⁴ The temperature dependence of the resistivity shown in Fig. 3 yields a slope of 0.20 eV which is less than the activation energy $E_1 = 0.22 \text{ eV}$ of the first acceptor level. This is due to the fact that hole mobility increases with decreasing temperature. Figure 4 shows the hole concentration versus temperature, and the slope of this plot yields the activation energy of the first level, which is found to be 0.22 eV above the valence-band edge. The hole drift mobility is deduced from the Hall mobility and the ratio R_H/R_∞ which ranges from 1.4 to 1.8 depending on the temperature and impurity concentration.^{13,14} The linear relationship between V_{PME} and $\Delta G/G_0$ is also observed for *p*-type samples, as is shown in Fig. 5 and predicted by Eq. (20).

For *p*-type samples, $p_0 \gg n_0$, also $p_1 \gg n_1$, from Eqs. (9) and (20), it is noted that the trapping ratio Γ has little effect on the values of V_{PME} and τ_n , also τ_{p01} can be ignored in the expression of τ_n . Thus, for *p*-type samples, we were unable to determine C_{p1} and γ_1 (where $\gamma_1 = C_{p1}/C_{n1}$) accurately. The relative importance of the recombination in both levels for this case depends not only on the resistivity of the samples, but also on the ratio of C_{n2}/C_{n1} . By varying the resistivity of the samples, which is achieved by changing the nickel-doping densities, we can obtain the ratio of C_{n2}/C_{n1} . From this result, we conclude that C_{n2} is larger than C_{n1} with the ratio of $C_{n2}/C_{n1} = 6$.

For samples with $p_0 < p_1$, the second acceptor level (i. e., E_2) dominates the recombination process, and τ_n is nearly equal to τ_{n02} . In this case, the value of C_{n2} obtained from the *p*-type samples agrees well with that obtained from *n*-type samples.

For samples with $p_0 > p_1$, the effect of the first acceptor level (i. e., E_1) becomes important. The value of C_{n1} can be determined from the PME and PC measurements. The result yields

$$C_{n1} = 1.4 \times 10^{-9} \text{ cm}^3 \text{ sec}^{-1}.$$

For comparison, the above result is also included in Table I.

IV. DISCUSSIONS AND COMPARISON WITH PREVIOUS WORK

In computing carrier capture rates from lifetime measurements for the nickel-doped germanium crystal, the reasons for the wide spread in the previous results may be attributed to the following facts: (1) experimental difficulties in determining accurately the density of electrically active nickel atoms; (2) failure to include the excess-carrier trapping effect in the PME theory; (3) improper assumptions on the temperature dependence of hole capture rates C_{p2} ; and (4) neglecting the term due to hole capture rates C_{p2} in the lifetime expression for *n*-type samples, which results in underestimating the electron capture rate C_{n2} at room temperature.

In an attempt to avoid all the possible errors cited above, we have employed a unique approach in determining the carrier capture rates for nickel-doped germanium crystals at room temperature. First, we have elaborately controlled the compensation ratio of nickel atoms and the shallow-impurity densities (see Sec. III) such that the density of nickel atoms can be measured accurately. Secondly, instead of computing capture rates from temperature dependence of lifetime data, we have determined the electron and hole capture rates at one single temperature (i. e., room temperature) in both *n*- and *p*-type samples; this has the advantage of eliminating possible errors arising from (3) discussed above. Thirdly, we have included the excess-carrier trapping effect in our PME and PC theory; our result has shown that the effect of trapping is more prominent in *n*-type crystals than in the *p*-type samples. Implications of the above criteria to our present work, as well as previous work, are discussed as follows.

The ratio of electron capture rates, C_{n1}/C_{n2} , obtained by us is $\frac{1}{6}$ at room temperature, which is in excellent agreement with that reported by Wertheim⁶ and Eliseev *et al.*,⁷ respectively. However, the values of C_{n1} and C_{n2} obtained here are somewhat higher than those obtained by Wertheim and Eliseev, while the value of C_{p2} obtained here is much lower than that of Wertheim, but agrees well with Burton *et al.*¹ This discrepancy can be explained by the following facts. Wertheim deduced the ratio of C_{n1}/C_{n2} from the two lifetime plateaus, one at low temperature (i. e., C_{n1}) and the other near room temperature (i. e., C_{n2}). Although C_{n1} is independent of temperature due to its neutral-center nature, it has been reported by Belyaev and Miselyuk¹⁵ that C_{n2} decreases with decreasing temperature for $140 < T < 280 \text{ }^\circ\text{K}$ due to Coulomb repulsion, and is essentially independent

of temperature for $280 < T < 350$ °K due to the tunneling penetration of the Coulomb barrier by electrons. The room-temperature value of C_{p2} reported by Wertheim was taken from his low-temperature-lifetime data by assuming that C_{p2} is independent of temperature. There has been no temperature-dependent data on C_{p2} reported as yet. However, it is expected that value of C_{p2} will decrease with increasing temperature due to its attractive-center nature.¹⁶ Thus, the value of C_{p2} reported by Wertheim at room temperature was overestimated, and C_{p2} should be less than 100×10^{-9} cm³ sec⁻¹ at $T = 300$ °K. In computing C_{n2} at room temperature from lifetime data for n -type crystals, Wertheim employed Eq. (1) of his paper and neglected the term due to C_{p2} . This results in underestimating the value of C_{n2} , because C_{p2} is not negligible at room temperature. In fact, we have substituted values of C_{n2} and C_{p2} , obtained in this paper, into Eq. (1) of his paper, and found that lifetimes computed from this result are in excellent agreement with his measured lifetimes for samples 532 at room temperature. Therefore, the value of C_{n2} reported by Wertheim is somewhat underestimated, while the value of C_{p2} deduced from his low-temperature data is overestimated at room temperature. Our present results support such conclusions.

Next, we examine the values of C_{n1} and C_{n2} reported by Eliseev and Kalashnikov.⁷ Their analysis of the lifetime data is essentially similar to that of Wertheim; however, they obtained values of C_{n1} and C_{n2} which are a factor of 2 lower than those of Wertheim. This is due to the fact that they determined C_{n1} and C_{n2} from the PME method, in which they failed to include the trapping effect in their PME theory. They pointed out that the lifetime data observed from the photoconductivity-decay experiment were only about 50~60% of their PME lifetimes. If we use the lifetime data they obtained from the photodecay experiment to analyze Eliseev's data, the results for C_{n1} and C_{n2} will be close to the values of ours. Thus, the values of C_{n1} and C_{n2} reported by Eliseev *et al.* are underestimated, which is due to the fact that they neglected the excess-carrier trapping effect in the PME theory.

Finally, the results of capture rates reported by Burton *et al.*¹ were obtained from lifetime data, which they determined from diffusion length measured over a wide range of conductivity at room temperature. Although the value of the hole capture rate reported by them agrees quite well with ours, it is noted that these data were available before the existence of the upper level had been recognized. The present result confirms that the hole capture rate due to upper level C_{p2} is equal to 40×10^{-9} cm³ sec⁻¹ at room temperature.

V. CONCLUSIONS

From the present study of the capture rates for nickel-doped germanium crystal determined by PME and PC methods at $T = 300$ °K, we conclude that (i) the ratio of C_{n1}/C_{n2} is equal to $\frac{1}{8}$, which is in good agreement with that of Wertheim and Eliseev *et al.* (ii) Our result yields $C_{n1} = 1.4 \times 10^{-9}$ cm³ sec⁻¹ and $C_{n2} = 8 \times 10^{-9}$ cm³ sec⁻¹; this result is consistent with Wertheim's result if C_{p2} was included in his Eq. (1) in computing C_{n2} from room-temperature lifetime data, and agrees well with the result of Eliseev *et al.* if the trapping effect was included in their PME theory. (iii) Our result for C_{p2} (40×10^{-9} cm³ sec⁻¹) is in excellent agreement with the value of Burton *et al.*, although their study was completed before the discovery of the upper level; the present result is also consistent with Wertheim's if his low-temperature data on C_{p2} were corrected to the room-temperature value without approximation. In short, we have demonstrated that by including the trapping effect in the PME and PC theory and by elaborately controlling the compensation ratios of nickel atoms and shallow-impurity densities, we are able to determine more accurately than previously three of the four capture rates for nickel atoms in germanium at room temperature from PME and PC measurements.

ACKNOWLEDGMENTS

This research is supported by the Advanced Research Project Agency and monitored by the AFRL under Contract No. F19628-68-0058.

¹J. A. Burton, G. W. Hull, F. J. Morin, and J. C. Severiens, *J. Phys. Chem.* **57**, 853 (1953).

²W. W. Tyler, R. Newman, and H. H. Woodbury, *Phys. Rev.* **98**, 461 (1955).

³J. F. Battey and R. M. Baum, *Phys. Rev.* **100**, 1634 (1955).

⁴J. Okada, *J. Phys. Soc. Japan* **12**, 471 (1957); **12**, 1338 (1957).

⁵S. G. Kalashnikov and K. P. Tissen, *Fiz. Tverd. Tela* **1**, 545 (1959) [*Sov. Phys. Solid State* **1**, 491 (1959)].

⁶G. K. Wertheim, *Phys. Rev.* **115**, 37 (1959).

⁷P. G. Eliseev and S. G. Kalashnikov, *Fiz. Tverd.*

Tela **5**, 320 (1963) [*Sov. Phys. Solid State* **5**, 233 (1963)].

⁸S. T. Sah and W. Shockley, *Phys. Rev.* **109**, 1103 (1958).

⁹S. C. Choo and A. C. Sanderson, *Solid State Electron.* **13**, 609 (1970).

¹⁰S. C. Choo, *Phys. Rev. B* **1**, 687 (1970).

¹¹W. Shockley and W. T. Read, Jr., *Phys. Rev.* **87**, 835 (1952).

¹²S. S. Li and H. F. Tseng, *Phys. Rev. B* **4**, 490 (1971).

¹³J. Wiley, in *Progress in Semiconductors*, edited by A. F. Gibson (Heywood, London, 1964), Vol. 8, Chap. 4,

pp. 96-131.

¹⁴M. B. Prince, Phys. Rev. **92**, 861 (1953).

¹⁵A. D. Belyaev and E. G. Miselyuk, Fiz. Tverd. Tela **6**, 2638 (1964) [Sov. Phys. Solid State **6**, 2101

(1965)].

¹⁶M. Lax, Bull. Am. Phys. Soc. **1**, 128 (1956); J. Phys. Chem. Solids **8**, 66 (1969).

PHYSICAL REVIEW B

VOLUME 6, NUMBER 8

15 OCTOBER 1972

Dependence of the Peak Energy of the Pair-Photoluminescence Band on Excitation Intensity

Eliam Zacks and A. Halperin

The Racah Institute of Physics, The Hebrew University of Jerusalem, Jerusalem, Israel

(Received 23 March 1972)

An analytical expression is derived for the dependence of the peak energy of the broad-band pair-recombination emission on the excitation intensity. Experimental values given in the literature were fitted by a nonlinear-least-square computer program to the theoretical expression. The fit gave values for the limiting photon energy for distant pairs ($h\nu_\infty$) and for the Bohr radius (R_B) for the shallow hydrogenic impurity in the crystal. Values obtained for GaP were $h\nu_\infty = 2.189$ eV and $R_B = 24.2$ Å (averages from two sets of experimental results). For ZnSe we obtained $h\nu_\infty = 2.691$ eV and $R_B = 28.1$ Å. The present method is specifically useful in crystals in which the discrete-line pair emission is not observable. It can, however, also help as a guide and a check in the classification of the discrete lines according to their shell number.

INTRODUCTION

The low-temperature photoluminescence due to donor-acceptor pair recombination has recently been widely studied. Hopfield *et al.*¹ have pointed out that for sufficiently distant pairs the dependence of the recombination energy $h\nu(r)$ on the pair separation r is given by the simple relation

$$h\nu(r) = E_g - (E_d + E_a) - E(r), \quad (1)$$

where E_g is the energy gap, E_d and E_a are the donor and acceptor ionization energies, and $E(r) = -e^2/\epsilon r$ is the Coulomb interaction energy of the pair. The observation of a series of fine emission lines in GaP and many other crystals having the zinc-blende structure²⁻⁷ proved in an unambiguous way that the emission in these crystals was due to pair recombination. Such line spectra have not as yet been clearly identified in crystals having other structures. Pair recombination in such crystals is therefore studied on the broad band, which is assumed to be formed by many closely packed lines due to recombinations of pairs with large separation r . This band emission has not been treated quantitatively until now. Thomas *et al.*² have examined the shift in the peak energy of the broad-emission band in GaP on changing the excitation intensity. They have plotted the logarithm of the excitation intensity against peak energies and have drawn a straight line through the widely scattered experi-

mental points. Maeda,⁸ again for GaP, did the same in spite of the clear deviation of the experimental points from the straight line. Dean and Merz⁵ carried out similar measurements on ZnSe. These authors, however, noted the deviation from a straight line and drew a curve through the experimental points.

In the present work an expression is derived for the dependence of the peak energy of the band on excitation intensity. The theoretical relation, when compared to experimental data gives values for the limiting photon energy of infinitely distant pairs ($h\nu_\infty = E_g - E_d - E_a$) and for the Bohr radius of the shallow hydrogenic impurity in the crystal.

THEORY

We consider a crystal of dielectric constant ϵ with donor and acceptor concentrations N_d and N_a , respectively, and with one of the impurities in minority, let us say $N_d \ll N_a$. We also assume that the temperature of the crystal is low enough so that thermal ionization of donors or acceptors is negligible. Any pair recombination will leave an ionized donor-acceptor pair of separation r , typically a nearest-neighbor pair. Excitation, e.g., by light producing band-to-band transitions, produces free carriers which eventually get captured by the ionized impurities and turns them back to the neutral state.

The intensity of the light emitted by recombination of pairs having separations between r and